SPINDLE SPEED REGULATION AND TRACKING IN INTERRUPTED CUTTING

by

TSU-CHIN TSAO, Assistant Professor
KIN-CHEOK PONG, Graduate Student

Department of Mechanical and Industrial Engineering
University of Illinois at Urbana-Champaign

ABSTRACT

The problem of precise speed regulation and tracking of spindle drive systems in interrupted cutting which generates spindle angle dependent disturbance torque is addressed. Three models of the direct-drive motor/spindle unit have been used for motor/drive sizing, controller design and numerical simulation purposes, respectively. A variable sampling time digital repetitive controller, which is triggered at fixed spindle rotation, has been designed in the spindle angle domain and implemented to demonstrate its effectiveness in compensating periodically varying dynamic loads.

INTRODUCTION

Precise speed regulation and tracking is desirable in interrupted cutting operations, which refer to intermittent tool and workpiece engagement in a cutting process. For instance, in the cut-to-length operation of web materials, a rotating cutter carries multiple blades to cut a moving web into specified length. To maintain tight tolerance, it is essential to precisely synchronize the cutter speed to the web feed. If a cutter with evenly spaced blades is required to cut the web to different lengths, the cutter speed must be precisely varied over one spindle rotation. In milling and intermittent turning/boring, such as turning a shaft with a keyway, constant cutting speed is desirable to maintain uniform surface finish and optimal tool life. Moreover, there are two potential applications of variable spindle speed tracking in milling. The first application is concerned with chatter suppression and the second application is concerned with cutter runout compensation.

Self-excited vibration called chatter is undesirable in machining operations. In milling, it has been recognized that chatter can be suppressed by using a cutter with uneven spaced inserts (Optiz et al. 1966, Doolan et al. 1975, Tlusty et al. 1983) or by varying the spindle speed periodically (Weck et al. 1975, Lin et al. 1988). Furthermore, it has also been suggested that forced vibration can be minimized by using an optimally spaced cutter (Doolan et al. 1976, Fu et al. 1984). Uneven insert spacing depends on the cutting conditions and workpiece geometry and lacks flexibility in adapting to changing conditions. Variable spindle speed has the advantage of programmability, overcoming the drawback of uneven insert spacing method. In order to achieve similar effect of uneven tooth spacing, the spindle speed must be varied periodically in every cutter rotation.

Runout that occurs in rotational machinery has undesirable effects on machining systems (Ber and Feldman 1976, Kline and DeVor 1983). It causes each cutting tooth to carry uneven chip loads resulting in non-uniform cutting force patterns. Excessively large forces on a particular insert can damage or break the cutting tooth and reduce the cutter life. Furthermore, a periodic peak force pattern occurring at the spindle rotational frequency may introduce an undesirable low frequency vibration to the machine tool, resulting in poor workpiece surface finish. Recently an approach to on-line cutter runout estimation has been developed(Gu et al. 1991). Precise tracking of a variable spindle speed or feedrate trajectory, which is generated based on the estimated runout, can compensate for the effect of runout. This is referred as indirect runout compensation. Tsao and co-workers (Tsao et. al. 1989, Tsao and Pong 1991) have proposed to vary the spindle speed to compensate for the effect of runout by direct cutting force feedback without runout compensation and demonstrated the feasibility by dynamic simulation. This is referred as direct runout compensation. For either indirect or direct approach, since the runout pattern repeats every spindle revolution, the spindle speed or feed rate must also be varied at the same rate.

All of the aforementioned interrupted cutting examples share two common characteristics. First, the spindle drive is subject to an intermittent cutting force (torque) waveform, which repeats every cutter revolution and has to be compensated by the motor torque in order to maintain desired speed. Second, when tracking a periodic speed trajectory, the driver has to generate a periodically varying spindle inertial load. The capabilities and limitations of spindle drives and controllers for such performance requirements have received little investigation except that Olbrich et al. (1985) did simulation studies of a linear quadratic optimal control system for varying spindle speed in face milling and concluded that varying spindle speed concept is feasible.

From the standpoint of controller design for the problem characteristics mentioned above, most existing control algorithms cannot render satisfactory performance. Traditional PID controller cannot do the job as integral action can only eliminate constant offset. Feedforward tracking control algorithm (Tomizuka 1987) cannot reject the unmeasurable periodic disturbances. Optimal control approaches, such as Linear Quadratic regulator, generally equalizes signals in all frequencies and does not take advantage of the periodic nature of the present problem, resulting in unsatisfactory performance. Special tracking algorithms like cross-coupled control (Koren 1980,1991, Kulkarni and Srinivasan 1990) are for multi-axes contour tracking, not applicable to the present single axis problem.

Repetitive control (Hara 1988, Tomizuka et al. 1990), which is capable of tracking or rejecting periodic disturbances perfectly based on internal model principle (Francis and Wonham 1975), seems particularly suited to address the current problem. However, it should be noted that the periodic behavior in the present problem is in terms of cutter spindle angle but not time. This aspect has been addressed by Tsao et al. (1989, 1991) by using spindle angle, instead of time, as the independent variable for repetitive controller design.

In this paper, we will address the motor/drive sizing from dynamic loading in variable speed interrupted cutting, present the angle domain digital repetitive control approach for precise spindle speed tracking and demonstrate the experimental results.

DYNAMIC MODELS OF MOTOR/SPINDLE DRIVES

Experimental System Description Figure 1 shows the schematic diagram of the face milling experimental system consisting of a brushless DC motor and a spindle connected by a disc-lign flexible disc coupling, a pulse width modulated (PWM) power amplifier, an analog velocity servo controller, a digital controller and a tachometer and an encoder connected to the rear motor shaft.. The digital control is implemented by an Intel 8096 based computer, which provides 10-bit resolution analog to digital conversion, 12-bit resolution digital-to-analog conversion and 8-bit up-down quadrature counters for motor encoder. This face milling system is a typical setup of direct spindle drive systems. Three motor/spindle drive dynamic models with increasing complexity are used for different purposes discussed next.

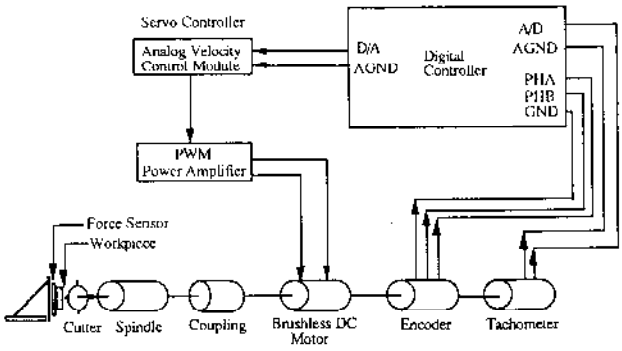

Figure 1 Experimental setup

Components	Parameters	Constants	Transfer Functions
Equivalent DC Brushless Motor/Spindle Drive	B J La Ra	0.02158 kg-m^2/s 0.04041 kg-m^2 0.0063 H 0.45 W	$\frac{1}{Js+B}$ $\frac{1}{La s+Ra}$
Torque Constant	$Cw1$	0.91 Nm/A	
Back e.m.f.	$Cw2$	0.91 Vs/rad	
Tachometer Gain	Cwt	0.0286 Vs	
Tachometer Dynamic $Fg(s)$	Tg	0.0004 s	$\frac{1}{T_g s+1}$
Velocity Loop Controller $Frw(s)$	Kpw Kiw	2.805 V/V 241.0 s^{-1}	$\frac{Kpw s+Kiw}{s}$
Current Feedback	Ki	0.05 V/A	
Current Loop Gain	Ku	13.0 V/V	
Current Loop Controller $Fri(s)$	Kpi Kii	240. V/V 1200000.0s^{-1}	$\frac{Kpi s+Kii}{s}$
Servo Controller gain	Kc	20 V/V	
Current Limit	$Iamax$	50 A	

Table 1: Motor/spindle drive parameters

Model for Component Sizing In interrupted cutting, The motor and its drive should be chosen such that required dynamic load can be produced. To this end, a simplified model can be used, which neglects the coupling spring compliance, the servo controller current loop dynamics and the tachometer dynamics:

$$J \frac{d\omega}{dt} = Te - Td - B\,\omega, \qquad (1)$$

For sizing motors and drives, the application's speed-torque (w-Te) curve, calculated from Eq. (1), must lie within the specified speed-torque region of the chosen motor. The application's peak and continuous torque should also be smaller than the specified values of the chosen motors and drives. For instance, speed regulation under dynamic load from interrupted cutting would require motor/drives to be able to generate the same cutting load. In speed tracking the rotational inertial load must also be included in the calculation of motor/drive size. It is easy to see that the rotational inertial load increase proportionally with the total inertia and the frequency and amplitude of speed variation.

Model for Controller Design For control system design of high bandwidth closed loop performance, the fast current loop and the tachometer dynamics should also be considered. Figure 2 shows the block diagram of this second model, in which $Fri(s)$ represents the transfer function of the current feedback controller. $Fg(s)$ is a first order transfer function representing the tachometer dynamics, $Gjb(s) = \frac{1}{Js+B}$, includes the inertial and damping loads, and $Frw(s)$ represents the servo amplifier's velocity PI controller. The transfer function from the command velocity input Uw^*, to the actual spindle speed output Wa, can be calculated from the motor data in Table 1. This model is of fifth order and is used for controller design.

Model for Simulation To get high fidelity to the actual system in numerical simulation , the third model further includes the coupling torsional spring between the motor shaft and the spindle shaft. The total inertia, J, of the spindle system consists of motor inertia J_1 and the spindle inertia J_2, as shown in Figure 3. Similarly, the lumped viscous damping B is broken into motor damping B_1 and spindle damping B_2. The coupling compliance is modelled as a torsional spring K. The inertia of the coupling is lumped into the motor inertia and the spindle inertia. The equations of motion are

$$Te - B_1 \frac{d\theta_1}{dt} - K(\theta_1-\theta_2) = J_1 \frac{d^2\theta_1}{dt^2} \qquad (2)$$

$$K(\theta_1-\theta_2) - B_2 \frac{d\theta_2}{dt} - T_d = J_2 \frac{d^2\theta_2}{dt^2} \qquad (3)$$

The transfer function from T_e to ω_1 can be calculated by taking the Laplace transform of Equation (2) and (3):

$$Gjb(s) = \frac{\omega_1(s)}{Te(s)} = \frac{J_2 s^2 + B_2 s + K}{J_1 J_2 s^3 + (J_1 B_2 + J_2 B_1) s^2 + [(J_1+J_2)K + B_1 B_2] s + (B_1+B_2)} \qquad (4)$$

The numerical values of J_1, J_2, B_1, B_2 and k are listed in Table 2. With this modification in $Gjb(s)$, the block diagram in Fig. 2 applies to this model identically. This model is of seventh order and is used in numerical simulation.

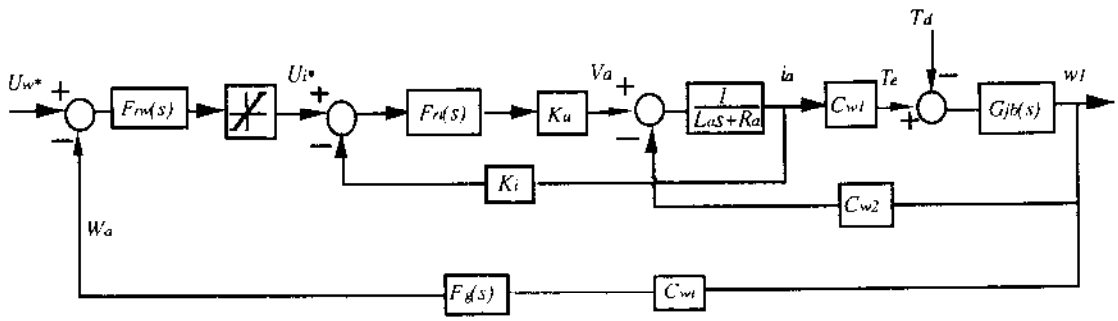

Figure 2 Block diagram of the motor/drive

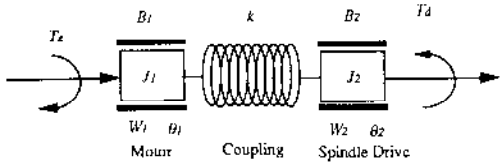

Figure 3 Coupling compliance schematic diagram

Motor Shaft Inertia	$J1$	0.01256 kg-m^2
Spindle Shaft Inertia	$J2$	0.02785 kg-m^2
Motor Viscous Damping	$B1$	0.015 N-m-s
Spindle Viscous Damping	$B2$	0.00658 N-m-s
Coupler Spring Constant	K	61828.3 N-m/rad

Table 2: Parameters for the model with coupling dynamics

Model Verifications Figure 4 shows the actual and the three models' frequency responses from the motor current command U_i* to the actual speed ω_{ri}. The first model has close agreement with the actual system from 0.01 Hz up to 30 Hz, the second model has close agreement up to 100 Hz, and the third model further characterizes the resonant and anti-resonant modes due to the coupling compliance. Figure 5 shows the close agreement in time domain step responses of the third model with the experimental results. It should be noted that the simulation was able to capture power amplifier current saturations, which accounts most for the system limitation in driving dynamic loads.

DIGITAL CONTROL SYSTEM

Variable Speed Tracking With PI Control We first show that the PI velocity controller is not capable of tracking time varying velocity profile. Consider a sine wave reference velocity profile composed of 40 points per period:

$$U\omega^*(kT) = \omega_0 + A\ sin(\frac{2\pi k}{40}).,\qquad (5)$$

where k is an integer index and T represents the sampling interval in terms of spindle angle, instead of time because of the nature of interrupt cutting aforementioned. Since the spindle speed will be varying, the sampling interval, which is fixed in angle, is actually varying in time. This makes it necessary to use the spindle encoder counts to trigger the sampling of the real-time software. The sampling interval used herein is 9 degrees, which make the sine wave profile in Eq. (5) repeats every spindle revolution.

Figure 6 shows the experimental results for tracking the sine wave angle function. The reference input at the first five revolutions is kept constant (300 rpm) and then is switched to the sine wave reference velocity profile with 120 rpm magnitude and 300 rpm nominal speed, resulting in about 100 rpm tracking error and -42 ~ 28 Amperes motor current oscillation.

Variable Speed Tracking with Repetitive Controller Repetitive control algorithm is proposed to track periodically changing velocity profiles. The detailed analysis of the stability of the repetitive controller can be found in Tomizuka et al.(1990). A brief summary of the repetitive controller design follows.

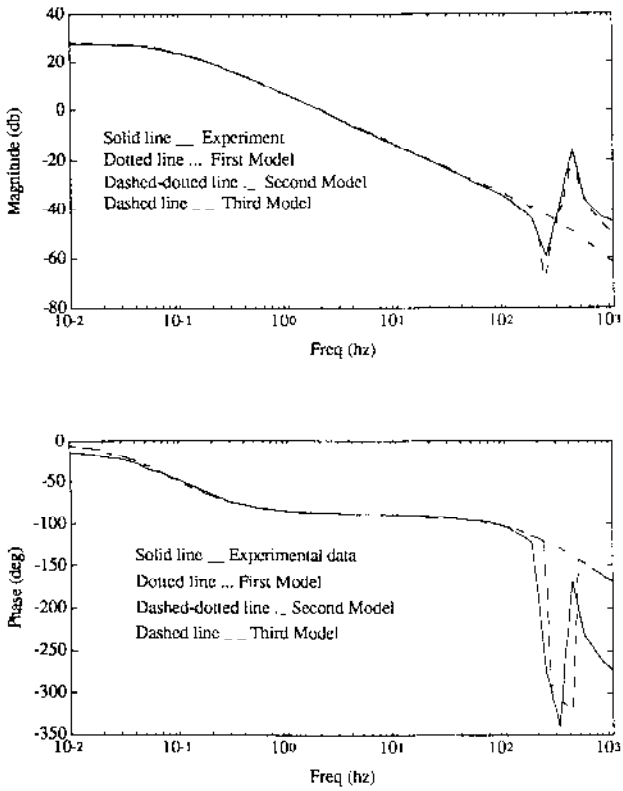

Figure 4 Frequency response plots

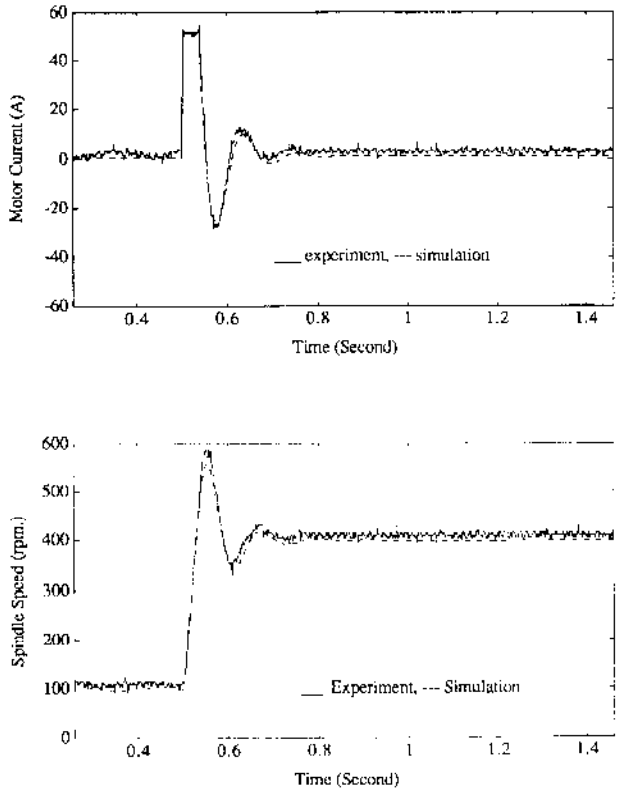

Figure 5 Step response plots

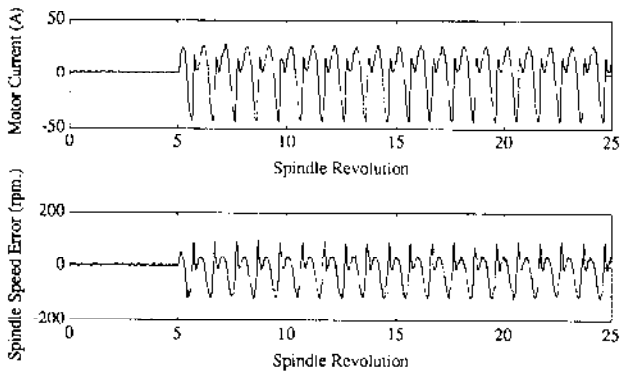

Figure 6 PI controller speed tracking performance

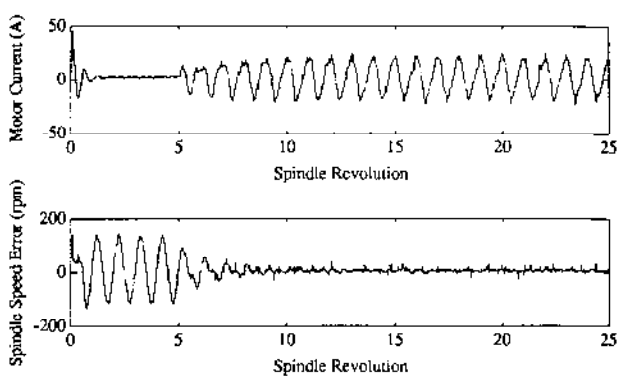

Figure 7 Repetitive controller speed tracking performance

Let the system discrete transfer function (from the command input, $U\omega^*$, to the measured speed output, ω_a) be

$$G(z^{-1}) = \frac{\omega_a(z^{-1})}{U\omega^*(z^{-1})} = \frac{z^{-d}B(z^{-1})}{A(z^{-1})} = \frac{z^{-d}B^+(z^{-1})B^-(z^{-1})}{A(z^{-1})}, \quad (6)$$

where z is the Z- transform variable of time and z^{-1} corresponds to a one step delay in the time domain; d is the delay of the process; $B^-(z^{-1})$ contains the zeros on or outside the unit circle and the undesirable zeros in the unit circle; $B^+(z^{-1})$ contains the zeros which are not in $B^-(z^{-1})$. The repetitive feedback controller has the following form

$$Gc(z^{-1}) = \frac{Ln\cdot R(z^{-1})\,F(z^{-1})}{S(z^{-1})(1-F(z^{-1})z^{-N})}, \quad (7)$$

$$\frac{R(z^{-1})}{S(z^{-1})} = \frac{z^{N+d+nu}A(z^{-1})z^{-nu}B^-(z)}{B^+(z^{-1})b}$$

$$b \geq max|B^-(e^{-j\omega})|^2$$
$$\omega \in [0,\pi]$$

where N is the number of sampling for one period of the disturbance; nu is the order of the polynomial $B^-(z^{-1})$; $B^-(z)$ is with z substituted for z^{-1} in $B^-(z^{-1})$; $F(z^{-1})$ is a low-pass filter ensuring robust stability (Tsao and Tomizuka 1988). It can be shown that the controller in Eq.(12) will be asymptotically stable and will asymptotically track periodic reference and reject periodic disturbance if $0 < Ln < 2$ (Tomizuka et al.1990).

By use of the "controller design model" and the numerical motor/spindle drive parameters listed in Table 1, the transfer function from $U\omega^*$ to Wa in the continuous-time domain is

$$G(s) = \frac{\omega_a(s)}{U\omega^*(s)}$$
$$= \frac{2.24e9s^2+1.14e13s+9.61e14}{s^5+2.73e4s^4+1.86e8s^3+3.12e11s^2+1.15e13s+9.61e14} \quad (8)$$

In order to design the repetitive controller in the angle domain, the plant model should also be represented in terms of angle (Tsao et al. 1989). To do so, first consider the state-space realization of the system. The state equations in time domain have the following form:

$$\frac{d\bar{x}}{dt} = [A]\,\bar{x} + [B]\,U\omega^* \quad (9)$$

$$\omega = [C]\,\bar{x}$$

where $\bar{x}$ represents the state variables such as spindle velocity w and motor current i_a; $[A]$ represents the process state matrix; $[B]$ represents the input matrix; $[C]$ is the output matrix. Dividing both sides of Eq.(9) by w, we get the state equation for the motor/spindle drive in the angle domain:

$$\frac{d\bar{x}}{d\theta} = \frac{1}{\omega}\{[A]\,\bar{x} + [B]\,U\omega^*\} \quad (10)$$

Equation (10) is a nonlinear system because ω is a state variable. To facilitate the repetitive controller design, which is based on a linear model, we linearize Eq.(10) at a nominal operating speed, ω_o. Denoting σ as the Laplace transform variable of the motor angle θ, we can derive the linearized model of Eq.(10) in transfer function form:

$$\delta\omega_a = G(\omega_o, \sigma)\;\delta U\omega^*, \quad (11)$$

where δ represents the variations from the nominal values. It is noted that the small signal transfer function from $\delta U\omega^*$ to $\delta\omega_a$ can be obtained simply by replacing s in Eq. (8) by $\omega_o\sigma$. If the nominal speed is 300 rpm, the transfer function from $\delta U\omega^*$ to $\delta\omega_a$ in the angle domain is as follows: (The variations δ is dropped hereafter for the convenience of presentation.)

$$\frac{\omega a(\sigma)}{U\omega^*(\sigma)} = \frac{7.22e4\sigma^2+1.17e7\sigma+3.14e7}{\sigma^5+870\sigma^4+1.88e5\sigma^3+1.0e7\sigma^2+1.19e7\sigma+3.14e7} \quad (12)$$

For 9 degree sampling interval, the system discrete transfer function with zero order hold is:

$$\frac{B(z)}{A(z)} = \frac{\omega_a(z)}{U\omega^*(z)}$$
$$= \frac{0.185z^4-0.101z^3-1.22e\text{-}2z^2+4.71e\text{-}9z+2.05e\text{-}24}{z^5-1.76z^4+0.836z^3-3.66e\text{-}6z^2+3.48e\text{-}21z-2.78e\text{-}37} \quad (13)$$

Here, z represents the Z-transform variable of spindle angle and z^{-1} corresponds to one-step delay in the angle domain; i.e. 9 degree delay.

By applying Eq.(7), the polynomials $R(z^{-1})$ and $S(z^{-1})$ can be found:

$$R(z^{-1}) = z^{-39}(1 - 1.76z^{-1} + 0.836z^{-2} - 3.66e\text{-}6z^{-3} + 3.48e\text{-}21z^{-4} - 2.78e\text{-}37z^{-5})$$

$$S(z^{-1}) = 0.185 - 0.101z^{-1} - 1.22e\text{-}2z^{-2} + 4.71e\text{-}9z^{-3} + 2.05e\text{-}24z^{-4} \quad (14)$$

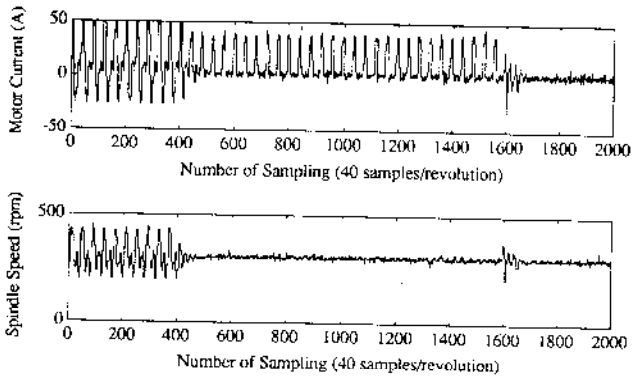

Figure 8 Repetitive controller speed regulation performance when in face milling

A low-pass filter $F(z^{-1}) = \frac{z + 2 + z^{-1}}{4}$ is applied in the controller, Eq. (7), to ensure robust stability against unmodeled dynamics, mainly the torsional spring of the coupling, and the angle domain nonlinear dynamics.

Figure 7 shows the experimental results of repetitive control for tracking the same velocity profile in Eq. (10). The repetitive controller is not turned on until at the end of the fifth revolution. The error signal converges to near zero within five revolutions and the motor current oscillation is within -20 ~ 24 amperes, smaller than that of the previous PI control case. Although the controller design is based on an approximate linearized plant model, the experiment results show that the closed loop system is stable and the tracking performance is far better than that of PI control. It should be noted that the repetitive controller is not only able to track periodic velocity profiles but it is also capable of rejecting periodic disturbances as occurred in interrupt cutting. This will be demonstrated by face milling examples in the next, where the interrupted cutting torque introduces a periodic disturbance to the system.

EXPERIMENTAL RESULTS IN FACE MILLING

Speed Regulation in Interrupted Flycutting The repetitive controller was applied to regulate the spindle speed in interrupted flycutting. Figure 8 shows the signals of the third case of a series experiments with four different cutting conditions listed in Table 3. The reference speed was set to 300 rpm. At the first ten revolutions, the analog PI control was intact and the repetitive controller was not activated. The spindle speed oscillated between 200 and 420 rpm. and the motor current saturated at 50 Amperes. The repetitive controller was activated after the tenth cutter revolution and the speed oscillation was eliminated in two cutter revolutions. Also noted is the graceful behavior as the cutter exits from the workpiece at around 1600th samples.

As an excursion from our subject, worth noting is that cutting torque and the cutting stiffness constant Kt can be easily estimated from the motor current when the cutting speed can be well regulated so that inertial load is eliminated. In this case, the left hand side of Equation (1) is zero:

$$Ia \cdot Cw_1 - T_{cut} - B \cdot \omega = 0 \qquad (15)$$

Assuming that there is only single tooth immersion, ,which is the case of fly cutting, the cutting torque, T_{cut} , equals to the tangential cutting force, F_t, times the cutter radius, R.

$$T_{cut} = F_t R \qquad (16)$$

Furthermore, the cutting force is dependent on the chip area by a proportional constant, the so called cutting stiffness constant:

$$F_t = K_t \cdot d \cdot f_t \cdot \sin(\theta), \qquad (17)$$

Test	f_t (mm)	d (mm)	ω (rpm)	ia_{max} (A)	K_t (N/m^2)
1	0.254	1.270	300	24	1.29e9
2	0.508	1.270	300	40	1.09e9
3	0.635	1.270	300	43	9.39e8
4	0.508	1.524	300	43	9.78e8

Table 3: Calculated cutting process gain for Aluminum 390

where Kt is the cutting stiffness constant, d is the depth of cut and ft is the cutter feed per tooth. Combining above equations we have

$$K_t = \frac{ia\ Cw_1 - B\ \omega}{d\ R\ ft\ \sin(\theta)} \qquad (18)$$

At the maximum tangential force, Eq.(18) can be simplified:

$$K_t = \frac{ia_{max}\ Cw1 - B\ \omega}{d\ R\ f_t} \qquad (19)$$

Table 3 shows the K_t computed for different cutting conditions by using this method.

Variable Speed Tracking in Interrupted Multi-Tooth Cutting The repetitive controller was applied to track the speed profile specified by Eq.(5) in interrupted multi-tooth (4-tooth) cutting. Figure 9 shows the experimental results with the nominal speed ω_0 at 300 rpm and the amplitude A = 50 and 125 rpm, respectively. The repetitive controller was not activated until the end of fifth revolution. For the case of tracking 50 rpm. amplitude wave, the speed tracking errors converged rapidly to near zero in four revolutions. For the case of 125 rpm. amplitude wave, the error converges to zero much slower mainly because the actual system now deviates from the small signal model assumed in the controller design. Note that the motor current wave forms generated by the repetitive controller not only have the one revolution period oscillation for generating the dynamic inertial load, but also have four ripples in every revolution for compensating the disturbance load from the four-tooth face milling. As can be expected, the periodic speed variation, which is synchronized with the cutter rotation, modulates the chip load and therefore can generate a runout like cutting force waveform. This is evident in Figure 10, in which the vertical cutting force (see Figure 1, in the direction normal to the feed axis and the spindle axis) is shown with the corresponding spindle speed waveforms. This also implies that the uneven chip load effect of cutter runout can be compensated by proper variable speed waveforms (Tsao and Pong 1990).

CONCLUSIONS

The purpose of this paper has been to demonstrate that precise speed regulation and tracking in interrupted cutting can be achieved by applying repetitive control algorithm. The following conclusions can be made from this study:

(1) Interrupted cutting has the characteristic of generating a cutter angle dependent periodic disturbance to the spindle drive. For precise speed regulation and tracking, the spindle drive and its control must be able to compensate this type of disturbance and (for tracking) dynamic inertial load.

(2) The limiting factors of motor/drives performance in precise speed tracking and regulation in interrupted cutting include motor/drive speed-torque curve, current loop performance and velocity loop performance. With the superior velocity loop performance of the angle domain repetitive controller presented in this paper and the fact that presently available current loop bandwidth is over 1000 Hz., the only limiting factor remained is the motor/driver speed-torque

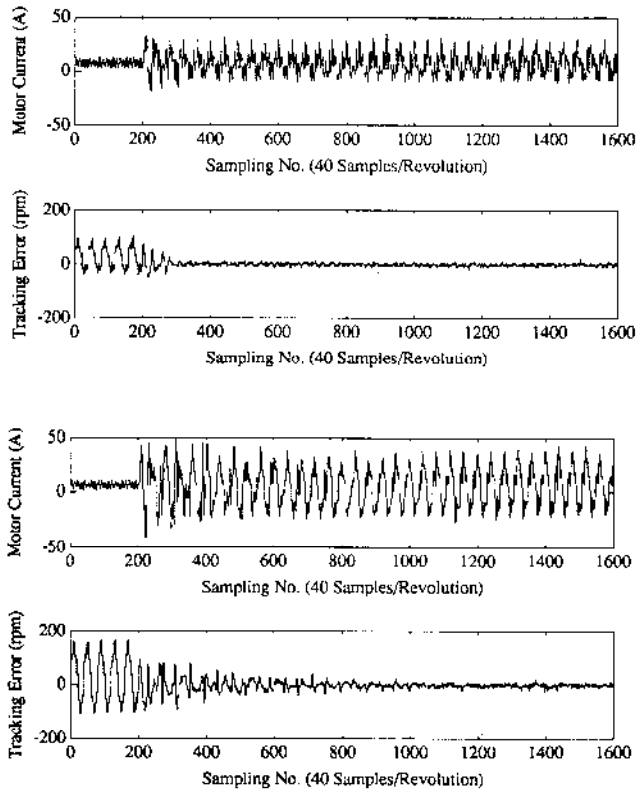

Figure 9 Repetitive controller speed regulation performance when in face milling (50 rpm amplitude: upper two traces, 125 amplitude: lower two traces)

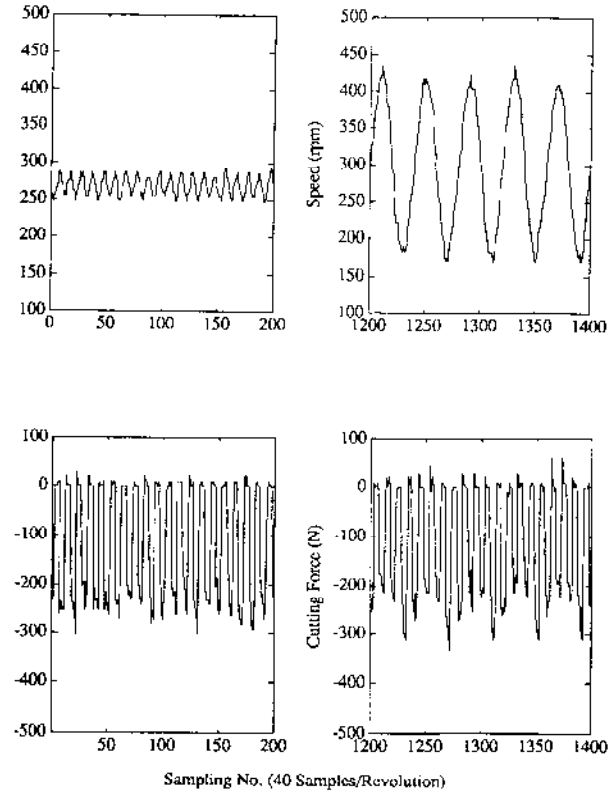

Figure 10 Vertical cutting forces modulated by the speed wave form (the case of 125 rpm amplitude)

capability. However this should not be a problem, even to the higher speeds and heavier cutting situations than what have been presented in this paper since large enough size motor/drives can be chosen. Therefore, the approach presented herein should be applicable to industrial heavy load interrupted cutting situations.

(3) Spindle angle domain digital repetitive control algorithm was presented, which effectively tracked and rejected spindle angle dependent periodic signals. Although the repetitive controller is derived based on a linearized small signal model, experimental results show that it can maintain the desired performance over a fairly large signal regime.

(4) Large speed oscillation over every spindle revolution can be achieved, implying that the concept of variable speed machining for programmable uneven insert spacing and for runout compensation can be implemented.

ACKNOWLEDGEMENT

This work was supported in part by National Science Foundation under Grant No. DDM 90-09830 and the University of Illinois Research Board computer time. The authors also wish to thank their colleagues Professor R.E. DeVor and Professor S.G. Kapoor for making their face milling research facilities available to this research.

REFERENCES

Ber A. and Feldman D., 1976, "A Mathematical Model of the Radial and Axial Throw of Square Indexable Inserts in a Face Milling Cutter," *Annals of CIRP.*

Doolan, P., M.S. Phadke and S.M. Wu, 1975, "Computer Design of a Vibration-free Face-Milling Cutter," *ASME Tran. Journal of Eng. Ind.* p. 925.

Doolan, P., F.A. Burney and S.M. Wu, 1976, "Computer Design of a Multipurpose Minimum Vibration Face Milling Cutter," *ASME Tran., J. of Eng. Ind.*,p.925.

Francis B.A. and W.M. Wonham, 1975, "The Internal Model Principle for Linear Multivariable Regulators," *Appl. Math. and Opt.*, Vol.2, p.170.

Fu, H.J, R.E. DeVor, and S.G. Kapoor, 1984, "The Optimal Design of Tooth Spacing in Face Milling Via a Dynamic Force Model," *Proc. of the 12th North American Manuf. Res. Conf.*, p.291.

Gu, F.,Kapoor,S.G.,DeVor,R.E., 1991, "An Approach to On-line Runout Estimation in Face Milling," *Tran. of NAMRI/SME*, p. 240.

Hara, S., Y. Yamamoto, T. Omata, and M.Nakano, 1988, "Repetitive Control System: A New Type Servo System for Periodic Exogenous Signals," *IEEE Tran. on Automatic Control*, vol. 33, no. 7, p.659.

Kline, W.A., and R.E. DeVor, 1983, " The effect of Runout on Cutting Geometry and Forces in End Milling," *Int. Jour. Mach. Tool Des. and Res.*, vol. 23, no. 2,1983, p.123.

Koren, Y., 1980, "Cross-Coupled Biaxial Computer Control for Manufacturing Systems," *ASME Tran., J. of Dynamic Systems, Measurement and Control*, Vol. 201, No.4, December, p.265.

Koren, Y. and Ch.-Ch. Lo, 1991, "Variable-Gain Cross-Coupling Controller for Contouring," *Annals of the CIRP*, Vol. 40/1, p.371.

Kulkarni, P.K. and K. Srinivasan, "Cross-Coupled Control of Biaxial Feed Drive Servomechanism, 1990, " *ASME Tran., J. of Dynamic Systems , Measurement and Control*, Vol. 112, No.2, June, p.225.

Lin, S.C., DeVor, R.E. and Kapoor, S.G., 1988, "The Effects of Variable Speed Cutting on Vibration Control in Face Milling," *ASME, Sensors and Control for Manufacture*, PED-Vol. 33, p.41.

Optiz, H., E.U. Dregger, and H. Roese, 1966, "Improvement of the Dynamic Stability of the Milling Process by Irregular Tooth Pitch," *Proc. Adv. MTDR Conf.*, p. 213.

Tlusty, J., Ismail, F. and Zaton, W, 1983, "Use of Special Milling Cutter Against Chatter," *Proc. of the 11 th North American Manufacturing Research Conference*, p.408.

Tomizuka, M., 1987, "Zero-Phase Error Tracking Controller for Digital Control, " *ASME Tran. J. of Dynamical Systems, Measurement, and Control*, Vol.109, p.65.

Tomizuka, M., T. C. Tsao, and K. Chew, 1989, "Analysis and Synthesis of Discrete-Time Repetitive Controllers," *American Society of Mechanical Engineers Journal of Dynamical Systems, Measurement and Control*, vol. 111, p.353.

Tsao, T., Burke, J. B. and Ferreira, P.M., 1989, "Control of Radial Runout in Face Milling," *Symposium on Control Issues in Manufacturing Processes*, ASME DSC- Vol.18, p.99.

Tsao, T.C. and Pong,K., 1991, " Control of Radial Runout in Multi-Tooth Face Milling," *Tran. of NAMRI/SME*, p.183.

Tsao, T.C and Tomizuka M, 1988, "Adaptive and Repetitive Digital Control Algorithms for Non-Circular Machining," *Proc. of the 1988 American Control Conference*, June, p.115.

Weck, M., Verhaag, E. and Gather, M., 1975, "Adaptive Control for Face-Milling Operations with Strategies for Avoiding Chatter-Vibrations and for Automatic Cut Distribution," *Annals of the CIRP*, Vol. 24, p.405.